CHAPTER 4

β-amyloid mediated nitration of MnSOD: Implication for oxidative stress in a APP^{NLh}/ APP^{NLh} x $PS\text{-}1^{P264L}$/ $PS\text{-}1^{P264L}$

Abstract

Alzheimer's disease (AD) is a multifactorial, progress-sive, age-related neurodegenerative disease. In familial AD (FAD), Aβ is excessively produced and deposited because of mutations in the amyloid precursor protein (APP), presenilin-1 (PS-1) and presenilin-2 genes. A double homozygous knock-in mouse model that incorporated the Swedish FAD mutations and converted mouse Aβ to the human sequence in APP and had the P264L FAD mutation in PS-1 was used. Aβ deposition was observed in double knock-in mice beginning at 6 months and also there was an increase in the levels of insoluble Aβ1-40/1-42. Brain homogenates from 3-, 6-, 9-, 12- and 14-month old mice showed that protein levels of manganese superoxide dismutase (MnSOD) were unchanged in the double knock-in mice compared to controls. Genotype-associated increases in nitrotyrosine levels were observed. Immunoprecipitation of these proteins revealed MnSOD as a target of this nitration. Although the levels of MnSOD protein did not change, MnSOD activity and mitochondrial respiration decreased in knock-in mice, suggesting a compromise in mitochondrial function. The compromised activity of MnSOD, a primary antioxidant enzyme protecting mitochondria, may explain mitochondrial dysfunction and provide the missing link between Aβ induced oxidative stress and AD.

Introduction

Alzheimer's disease (AD) is a multifactorial progresssive, age-related neurodegenerative disease that affects over four million persons in the USA (Evans et al. 1989). The pathological hallmarks of AD are extracellular Aβ deposits, neurofibrillary tangles, synaptic loss, and neuronal degeneration. Aβ plaques are composed of 40 and 42-mer peptides (Aβ1-40 and Aβ1-42) that are proteolytically produced from APP (Iwatsubo et al. 1994). Three genes, presenilin 1 (PS-1), presenilin 2, and APP are causatively linked with the pathogenesis of early onset familial AD (FAD). The findings that Aβ is central to the pathogenesis of AD (Selkoe et al. 2001) and that the AD brain is under significant oxidative stress were united into a comprehensive model for neurodegeneration in the brain in AD based on Aβ-associated free radical generation (Butterfield et al. 2002). The brain in AD has marked oxidative damage as manifested by increased protein oxidation, lipid peroxidation, free radical formation (Butterfield et al. 2002), 3-nitrotyrosine (3-NT) levels (Smith et al. 1997, Castagna et al. 2003), advanced glycation end products (Butterfield et al. 2001) and DNA/RNA oxidation products (Mecocci et al. 1991, Numomura et al. 1999).

MnSOD is a homotetramer consisting of identical 24-kDa subunits. The translated precursor in cytosol contains an N-terminal 24 amino acid sequence signaling mitochondrial compartmentalization. The mature protein protects the cells against cytotoxic $O_2^{\cdot-}$. The importance of this enzyme is evident from MnSOD "knockout" mice that suffer from a defect of mitochondrial iron-sulfur centers, a modification proving lethal to newborns (Lebovizt et al. 1996, Li et al. 1995). Activity of this antioxidant enzyme declines in the aging process (Wei et al. 2002). Because the AD brain is under intense oxidative stress, any dysfunction of MnSOD may lead to progression of the disease.

Peroxynitrite anion ($ONOO^-$) is a potent biological oxidant that has been implicated in diverse forms of free radical induced tissue injury (Wiseman et al. 1996). Peroxynitrite is produced by the reaction of $O_2^{\cdot-}$. and $^{\cdot}NO$, and this ONOO- can compromise the functional and/or structural integrity of target proteins (Beckman et al. 1996). Increased levels of nitrotyrosine (Smith et al. 1997) and 4-hydroxynonenal (HNE) (Montine et al. 1997) are associated with degenerating

neurons in AD, suggesting pathogenic roles of ONOO- and membrane lipid peroxidation in this disease.

Mutations in the APP gene and PS-1 gene lead to increased levels of Aβ, which appear to contribute to the disease process. One study demonstrated altered levels of Aβ1-40 and Aβ 1-42 distinguish AD from normal aging (Games et al. 1995). Recently several transgenic animals have been shown to have increased Aβ peptide deposition and some of the pathologic characteristics similar to AD patients (Wang et al. 1999, Hsia et al. 1999). Crossing APP-Tg mutant mice and PS-1-Tg mutant mice resulted in increased Aβ production and accelerated amyloid deposition in the brain of these animals (Borchelt et al. 1997, Holcome et al. 1998). However, increased Aβ levels in these models may, in part, be due to an increase in copy number of the transgenes.

The aim of this study was to use a mouse model that resembles the natural progression of Aβ pathology similar to that observed in AD patients and to gain an insight into potential causes of the mitochondrial alterations that occur during the progression of AD. The model that we used is a homozygous knock-in $APP^{NLh/NLh}$ X PS-$1^{P264L/P264L}$ (APP/PS-1) (Reaume et al. 1996). The results presented here demonstrate that these mice have an age-dependent accumulation of Aβ in the brain, which is consistent with an increase in both Aβ1-40 and Aβ1-42 and an accelerated decline in mitochondrial function associated with a decrease in activity of MnSOD due to nitration. These results suggest a novel Aβ-mediated nitrative inactivation of MnSOD and inhibition of mitochondrial function in AD.

Materials and Methods

Mutant mouse lines:

APPNLh/NLhXPS-1P264L/P264L mutant mice were generated using the Cre-lox© knock-in technology (Reaume et al. 1996, Holcomb et al. 1998). The APP strategy introduced the Swedish FADK670N/M671L mutations and changed the mouse sequence for Aβ to be identical to the human sequence (NLh). These mice demonstrate proper cleavage of the APP protein to generate the Aβ peptide. The PS-1 mutation targeted codons 264 and 265 of the mouse PS-1 gene to introduce the proline to leucine (P264L) mutation. When PS-1 mutant mice (P264L) are crossed with the mutant APP mice (NLh), the mutations are driven by the endogenous promoters of the APP and PS-1 genes and expression is limited to the replacement of these two endogenous genes and not by the expression of multiple transgenes.

Genotyping of mice

APP/PS-1 mice were maintained on a CD-1/129 background. Wild type (WT) mice were obtained from heterozygous APP/PS-1 matings and maintained as a separate line for use as controls. The APP/PS-1 mutant mice were monitored for maintenance of the knock-in gene by PCR analysis of tail snip DNA (Reaume et al. 1996). The APP NLh mutation was screened with primers spanning the lox^{p} sequence in intron 15 of the targeted locus (5'-CACA-CCAAGAAGTACAATAGAGGG-3' and 5'-CCTGGGTTGTA-GGGACTGTACTTG-3') (Invitrogen, CA). Wild type mice showed a single band at 214 bp, while the homozygous mutant mice had a single band at 298 bp. The PS-1 P264L mutation was identified using primers spanning exon 8 (5'-CCCGTGGAGGTCAGAAGTCAG-3' and 5'-TTACGGGTTGAGCCATGAATG-3') (Lamb et al. 1999) (Invitrogen). Wild type mice showed a single band at 142 bp, while the homozygous PS-1 knock-in mutant mice showed a single band at 219 bp. The mice used in all experiments were either WT or homozygous for APP/PS-1 mutation.

Immunocytochemistry for Aβ

To determine the deposition of Aβ in APP/PS-1 mice, one brain hemisphere from 3-, 6-, 9-, 12- and 14-month old mice was fixed in 4% formaldehyde, processed in the standard manner, embedded in paraffin and sectioned at 10 μm thickness. The sections were deparaffinized, hydrated and immersed in 88% formic acid for 3 minutes and washed in distilled water. Following blocking with 15% filtered horse serum in automation buffer (Biomeda Corp., CA) for 1 hour at room temperature, the sections were immunostained with 10D-5 monoclonal antibody (1:100) (NCL-B-Amyloid) and a biotiny-lated anti-mouse IgG secondary antibody (Vector Labs, CA). The sections were developed using an ABC reagent kit (Vector Labs) and counterstained with hematoxylin.

Tissue preparation for Aβ ELISA

Cerebral cortices were serially extracted with Tris-buffered saline (TBS), pH 7.4, followed by RIPA buffer (0.5% sodium deoxycholate, 0.1% SDS, 1% NP40, and 5 mM EDTA in TBS) and finally in 70% formic acid. Protease inhibitor cocktail (pepstatin A, leupeptin, TPCK, TLCK, soybean trypsin inhibitor, 1 μg/ml of each in 5 mM EDTA) was added during TBS and RIPA extraction. To measure the levels of Aβ1-40 and Aβ1-42 the supernatant obtained from the SDS extraction step was analyzed by ELISA.

Sandwich ELISA to determine the levels of insoluble brain Aβ1-40 and Aβ1-42

The sandwich ELISA used here was performed as described previously (Skovronsky et al. 1998, Turner et al. 1996, Suzuki et al. 1994) and the absorbencies falling within the standard curve for each assay were converted to picomoles. The sandwich ELISA consisted of a capture monoclonal antibody (MAb; BAN50) that was specific for the first 10 amino acids in Aβ and was used in conjunction with one of two different detection antibodies, BA27 MAb specific for Aβ species ending at amino acid 40 or BC05 MAb that is specific for Aβ species ending at position 42 (43). This ELISA had a detection limit of 3 to 6 fmol/well for Aβ1-40 and 1-42/43. The MAbs

BAN50, BA27 and BC05 were prepared as described previously and each ELISA result was normalized for the dilution and tissue weight (pmol/μg wet tissue).

Mitochondrial isolation

Mice were euthanized; brains (excluding cerebellum) of three mice from each age group were pooled, homogenized in 5 ml of ice-cold mitochondrial isolation buffer containing 0.225 M D-mannitol, 0.075 M sucrose, 20mM HEPES, 1 mM EGTA and 1% bovine serum albumin, pH 7.2 in a Dounce homogenizer with a glass pestle. The homogenized brains were then diluted with isolation buffer to a final volume of 10 ml, centrifuged at 1,500×g for 5 minutes. The supernatant was kept on ice, and the pellet resuspended in 3 ml of isolation buffer, homogenized and centrifuged at 1,500×g for 5 minutes. The supernatants were combined and centrifuged at 13,500×g for 10 minutes. The brown mitochondrial pellets were resuspended in 100 μl of isolation buffer and kept on ice, and the protein concentration was determined by Bradford assay.

Measurement of mitochondrial respiration

Mitochondrial proteins were resuspended in buffer containing 0.25 M sucrose, 50 mM HEPES, 2 mM $MgCl_2$, 1 mM EGTA, 10 mM KH_2PO_4 and 0.5% bovine serum albumin, pH 7.4. Oxygen consumption was measured using a Clark-type electrode oxygraph (Hansatech Inc., UK) with 10 mM pyruvate and 5 mM malate as substrate in the absence of exogenous ADP (state 2 respiration) and after addition of 300 mM ADP (state 3 respiration). The ATPase inhibitor oligomycin (100 μ g/ml) was then added to inhibit mitochondrial respiration. In normally coupled mitochondria, the addition of oligomycin slows respiration to a rate similar to that of state 2, whereas in uncoupled mitochondria oligomycin inhibition is reduced. Respiratory control ratio (RCR) was calculated as the ratios between state 3 and state 2 respirations.

Immunoprecipitation

Isolated mitochondrial protein (200 µg) was resuspended in 200µl RIPA buffer (9.1 mM Na_2HPO_4, 1.7 mM NaH_2PO_4, 150 mM NaCl, 0.5% sodium deoxycholate, 1% v/v Nonidet P40, and 0.1% sodium dodecyl sulfate, pH 7.2). Polyclonal nitrotyrosine antibody (anti-rabbit, 2 µg/ml, Cayman Chemical, MI) was added and incubated overnight at $4^{O}C$. Protein A/G agarose (20 µl) (Santa Cruz, CA) was added to the mixture and incubated overnight. Immunocomplexes were collected by centrifugation at 1,000×g for 5 minutes at $4^{O}C$, followed by washing with RIPA buffer, 4 times. Immuno-precipitated samples were recovered by resuspending in 2x sample loading buffer, and immediately fractionated by reducing SDS/PAGE and analyzed by Western blot. Positive control, homogrnated protein + 2 mM ONOO-; ONOO- was provided by Dr. Timothy R. Miller, Graduate Center for Toxicology, University of Kentucky, Lexington, Kentucky.

Western blot analysis

Equal amounts of brain homogenate proteins were resuspended in 2x sample loading buffer and separated on 12.5% SDS-PAGE. Proteins after separation by SDS/PAGE were transferred electrophoretically to nitrocellulose membranes (Schleicher & Schuell, Germany) and blocked with 5% nonfat dried milk in 50 mM Tris, pH 7.9, 150 mM NaCl and 0.05% (v/v) Tween-20. After blocking, the blots were incubated overnight at $4^{O}C$ with appropriate primary antibody (rabbit, anti-MnSOD IgG, dilution 1:10,000, Upstate, NY), followed by incubation with horseradish peroxidase-conjugated anti-rabbit secondary antibody. Probed membranes were washed three times and immunoreactive proteins were detected using enhanced chemiluminescence (ECL; Amersham Corp., NJ).

MnSOD activity assay

SOD activity in the homogenized brain sample was measured by the nitroblue tetrazolium (NBT)-bathocuproine sulfonate (BCS) reduction inhibition method (Spizt and Oberley

1989). This is an assay based on the competition reaction between SOD and the indicator molecule, NBT. When increasing amounts of protein (containing SOD activity) were added to the system, the rate of NBT reduction was progressively inhibited. Potassium cyanide at 5 mM was used to inhibit Cu/ZnSOD and thus measured only MnSOD activity. The assay mixture also contained catalase to remove H2O2 and diethylenetriamine-pentaacetic acid (DETAPAC) to chelate metal ions capable of redox cycling and interfering with the assay system. One unit of SOD activity was defined as that amount of SOD protein that caused a 50% reduction in the background rate of NBT reduction.

Statistical analysis

Statistical significance was analyzed by two-way ANOVA, followed by Newman-Keuls multiple comparison test when applicable. The experiments were repeated at least three times and the graphs were drawn using Graph Pad Prism, Version 3.02.

Results

Aβ deposition in APP/PS-1 mice

To determine the deposition of Aβ, we examined brain sections that were immunostained with 10D-5 antibody (Figure 4.1). The brains from WT mice contained no plaques at any age. The APP/PS-1 animals showed no deposition of Aβ at age of 3 months (Figure 4.1A). At the age of 6 months (Figure 4.1B), a few microscopic, scattered, small Aβ plaques were found in the frontal cortex. By 9 months (Figure 4.1C) there were a few larger Aβ plaques and more scattered smaller Aβ deposits. By 12 months (Figure 4.1D), Aβ deposition was more prominent in the neocortex and spread of plaques to the hippocampus occurred, with many larger confluent Aβ plaques and many small and moderate size plaques. By 14 months, there were larger numbers of Aβ deposits and Aβ in small blood vessel walls in brain and leptomeninges. These results suggest that there was an age-related, regional dependence to Aβ deposition in APP/PS-1 mice (Conducting pathology test by Professor William R. Markesbery).

Increased levels of Aβ1-40 and 1-42 fractions in APP/PS-1 mice

The accumulation of diverse species of Aβ peptides in amyloid plaques is a multistep process including the conversion of soluble Aβ into insoluble derivatives that assemble into amyloid fibrils and aggregate in extracellular deposits (Games et al. 1995). We examined whether the APP/PS-1 mice model showed an increase in levels of SDS soluble fractions of Aβ1-40 and 1-42 in cerebral cortical tissue. APP/PS-1 mice exhibited a trend of age-related increase in the load of both species of Aβ(Figure 4.2) (Conducting by Micheal P. Murphy and Dr. Jeferry N. Keller).

Unchanged MnSOD protein levels in WT and APP/PS-1 mice

Expression of MnSOD is highly inducible by oxidative stress inducing agents. To determine whether increases in Aβ produced increases in MnSOD enzyme levels, Western blot

analyses of brain homogenate from animals of different ages of both WT and APP/PS-1 mutant mice were performed. The protein levels of MnSOD did not change when compared between genotypes or between different ages within a genotype (Figure 4.3).

Increased nitration of MnSOD in APP/PS-1 mice

MnSOD is susceptible to peroxynitrite induced inactivation (MacMillan-Crow et al. 1996). To determine if Aβ-induced oxidative stress was associated with nitration and inactivation of MnSOD, nitration of MnSOD was detected by Western blot analysis of SDS/PAGE fractionated mitochondrial proteins, which had been immunoprecipitated using a polyclonal anti-nitrotyrosine antibody. Immuno-detection with polyclonal anti-MnSOD demonstrated detectable levels of nitrotyrosine in WT mice at all ages tested. In contrast, the APP/PS-1 mice showed an increasing trend in the level of immunoreactive-nitrated MnSOD (Figure 4.4A, 4.4B), but the increase was not statistically significant at $p < 0.05$. The increase was significant when compared between the two genotypes ($p < 0.01$).

Decreased SOD activity in APP/PS-1 mice

MnSOD catalyzes the dismutation of superoxide to hydrogen peroxide and molecular oxygen and this conversion was used to estimate the activity of MnSOD. The activity of MnSOD in APP/PS-1 mice was significantly decreased ($p < 0.0001$) when compared to the WT mice. Wild type mice showed a significant (**$p < 0.05$) decrease in MnSOD activity at 12 and 14 months when compared to 3-month old mice of their own genotype (Figure 4.4C). There was also a significant decrease (*$p < 0.05$) in activity of MnSOD in APP/PS-1 mice when compared to their age-matched WT controls (Figure 4.4C).

Decreased mitochondrial respiration in APP/PS-1 mice

MnSOD is a primary antioxidant enzyme protecting mitochondria from oxidative injury. To determine whether a reduction of MnSOD activity would affect the mitochondrial

respiratory function, oxygen consumption by isolated mitochondria was measured as an indicator of the mitochondrial respiration activity. Pyruvate and malate were used as substrates to determine the function of brain mitochondria from wild type and APP/PS-1 mice via complex I respiration. The results showed that the respiratory control ratio (RCR) of mitochondria was significantly (*$p < 0.01$) decreased in 9- and 12-month old APP/PS-1 mice when compared to age-matched WT mice and also when compared to 3-month old mice of both genotypes (**$p < 0.001$) (Figure 4.5). The results suggest that in APP/PS-1 mice there is inhibition of NAD-linked state 3 respiration rate, which is mediated through complex 1 of the mitochondrial electron transport chain. Wild type mice showed a small decrease in mitochondrial respiration with age, however, it was not statistically significant.

Discussion

Numerous reports have described attempts to recapitulate the hallmark pathologies of AD in the rodent brain by overexpression of human APP or APP fragments in transgenic models (Games et al. 1995, Lamb et al. 1993, LaFerla et al. 1995). Examples include, Tg2576 mice that over express human APP695 (Hsiao et al. 1996) with Swedish FAD mutations, mice obtained by crossing Tg2576 mice and transgenic PS1-P264L mice (Holcomb et al. 1998, McGowan et al. 1999) and the crosses of other Swedish APP transgenic mice with transgenic FAD mutant PS-1 mice (Borchelt et al. 1997, Lamb et al. 1999). In this study, we used a double gene-targeted APPNLh/NLh/PS-1P264L/P264L mouse model for amyloid deposition without the overexpression of APP (Flood et al. 2002).

Humanization of the mouse Aβ gene sequence results in an approximate 3-fold increase in amyloidogenic processing of recombinant APP in rat hippocampal neurons infected with Semliki Forest Virus expression constructs (DeStrooper et al. 1995) and single mutant PS-1 allele was sufficient to elevate the concentration of Aβ1-42 in brain and speed the onset of amyloid deposition and reactive astrogliosis (Siman et al. 2000). Our results using mice homozygous for APP/PS-1, which completely lack wild type APP or PS-1 and expressed both mutant FAD APP and PS-1 at natural levels, showed age-dependent increases in amyloid pathology (Figure 4.2) in accordance with the results obtained from APP 695SWE transgenic mice having PS-1 P264L knock-in mutation (Siman et al. 2000, Skovronsky et al. 1998). The observed accelerated Aβ deposition in APP/PS-1 mice also seems to have regional dependence in relation to age, with deposition seen first in frontal cortex and later encompassing other cortical regions and hippocampus. Thus, this humanized mouse model should serve as a useful model to study the Aβ-induced pathology in human AD.

Measurement of Aβ1-40 and 1-42 showed that there was an increasing trend in both species in APP/PS-1 mice. Our findings are in concordance with that of Wang et al (1999). who demonstrated an increase in average levels of Aβ1-40 and Aβ1-42 in AD. Our finding of increased quantity of Aβ1-40 and Aβ1-42 is consistent with the possibility that Aβ1-42 serves as the initial

seeding event for plaque formation and that increased levels of Aβ1-40 play a role in growing plaques and may be mechanistically linked to the onset and progression of AD (Wang et al. 1999).

The AD brain is under pronounced oxidative stress, as manifested by protein oxidation, lipid peroxidation, DNA and RNA oxidation, widespread peroxynitrite-induced damage, advanced glycation end products, and altered antioxidant enzyme expression. Aβ, in ways that are inhibited by antioxidants such as vitamin E, causes brain cell protein oxidation, lipid peroxidation and ROS formation, among other oxidative stress responses, suggesting that this peptide is a source of oxidative stress in brain (Butterfield et al. 2001). Other sources of oxidative stress in AD are likely, ranging from altered mitochondrial function, trace metal ion imbalances to binding of altered metal ion to biomolecules (Markesbery 1997). Our results that indicate increased nitration of MnSOD protein signify an increase in oxidative stress in the brain of the APP/PS-1 mice and suggest a compromise in mitochondrial function of APP/PS-1 mice due to increased oxidative stress.

The mitochondrion, a major subcellular source of ROS (Dugan et al. 1995, Piantadosi et al. 1996) plays a pivotal role in apoptosis (Kroemer et al. 1997). But the mitochondrion is also a site of cellular protection against ROS that involves an elaborate antioxidant defense system, especially MnSOD. Our studies indicate that the expression pattern of MnSOD in APP/PS-1 mice remained unaltered in all age groups, but SOD activity in APP/PS-1 mice was significantly reduced when compared to age-matched WT mice suggesting that the protein was inactivated. Our finding is in accordance with that reported by Macmillan-Crow et al. (1996) in a chronic rejecting renal model. The decreased activity of MnSOD is due to nitration of tyrosine residues (Smith et al. 1996, 1997), that occurs on the MnSOD protein. Tyrosine nitration (3-nitrotyrosine, 3-NT) is an in vivo posttranslational protein modification with potentially significant biological implications (Beckman 1996, Ischiropoulos et al. 1998) and has been detected in a number of human and animal models of disease (Kroemer et al. 1997). 3-NT is increased in the hippocampus and cerebral cortex of aged rats (Shin et al. 2001), the CSF of aged humans (Tohgi et al. 1999) and the subcortical white matter of aged monkeys (Sloane et al. 1999). 3-NT formation is the hallmark of reactive peroxynitrite (ONOO-) and this modification can compromise the functional and/or structural integrity of target proteins (Smith et al. 1996) especially MnSOD (Ischiropoulos et al. 1992). NO, after diffusing into mitochondria can inhibit oxygen consumption by complex IV. Inhibition by .NO is reversible,

however, this process decreases electron transport and could potentially increase the concentration of O_2-. (MacMillan-Crow et al. 1996). MnSOD has a function to eliminate O_2-. from the mitochondrial matrix space. But, the concentration of .NO required to inhibit complex IV is sufficient to compete effectively with MnSOD for O_2-. by a rapid reaction generating peroxynitrite, which can nitrate tyrosine residues and inactivate MnSOD to increase further the intramitochondrial level of O_2-. (MacMillan-Crow et al. 1996). O_2-. reacts with NO faster than with MnSOD (Hsu et al. 1996), therefore, if mitochondria contain inactive MnSOD, this peroxynitrite can further nitrate MnSOD and inactivate MnSOD to increase the intramitochondrial level of superoxide. Consequently this peroxynitrite-mediated amplification cycle would result in a progressive increase of mitochondrial levels of peroxynitrite, which can induce additional cytotoxic effects (MacMillan-Crow et al. 1996) including inactivation of complexes I and II in the mitochondrial respiratory chain (Cassina et al. 1996).

Myeloperoxidase (MPO), one of the principal hemo-proteins stored in the azurophilic granules of neutrophils and lysosome of monocytes, is also a catalyst of nitrotyrosine formation via nitrite oxidation to the potent nitrating species nitrogen dioxide (.NO2) (Baldus et al. 2001). It has been proved in vascular tissues that MPO significantly contributes to nitrotyrosine formation in vivo (Baldus et al. 2001, 2002). Further, it has been shown that MPO-/- animals have reduced nitrotyrosine immunoreactivity than WT mice (Baldus et al. 2002). Myeloperoxidase is not only present in neutrophils and monocytes, but also in microglia. Microglia are quiescent in normal brain but can become activated in response to neuronal damage or various other stimuli, including aggregated Aβ (El Khoury et al. 1998, Meda et al. 1995). In AD, MPO has been shown to be colocalized around the Aβ plaques, and also in microglia-macrophages that are present around the plaques. It has also been shown that Aβ treatment of mouse microglia cell line BV-2 resulted in strong induction of MPO mRNA expression (Reynolds et al. 1999). From these observations and the fact that senile plaques are surrounded by activated microglia, it can be cautiously speculated that MPO may also contribute to the nitration of MnSOD.

Despite major advances in the study of nitration of proteins, the effect of nitration on protein turnover and the pathways that degrade the nitrated proteins have not been fully elucidated. There are reports about faster degradation of proteins treated with ONOO- or a generator of nitric

oxide and superoxide by 20S proteasome (Grune et al. 1998). Consistent with this, Souza et al. (2000) reported that a single nitrating event is sufficient to target proteins for degradation by the proteasome. Although protein nitration is generally viewed as an irreversible event, "activities" that appear to specifically repair nitrated proteins have been reported in human and rat tissues (Gow et al. 1996, Kamisaki et al. 1998). Thus it tempting to speculate that nitration of MnSOD may be reversible. In this regard, our APP/PS-1 mouse model is ideal for testing pharmacological intervention by mitochondrially targeted antioxidants such Mito-Q or Mito-Vit E.

Mito-Q [mixture of mitoquinol – 10 - (6' – ubiqui-nolyl) decytriphenylphospho nium and mitoquinone - 10 -(6' – ubiqui nonyl) decyltriphenylphosphonium] (Kelso et al. 2001) and MitoVit E [2 - [2 - (triphenylphosphonio) ethyl] - 3, 4 - dihydro - 2, 5, 7, 8 - tetramethyl - 2H - 1 - benzopyran - 6 - ol bromide] (Echtey et al. 2002) have been found to destroy superoxide in the mitochondrial matrix (Echtey et al. 2002). Mito-Q (Mito-Q10) has been shown to be an effective antioxidant against lipid peroxidation, peroxynitrite and superoxide (James et al. 2005). Pretreatment with Mito-Q and Mito Vit-E have been shown to i) significantly abrogate the lipid peroxide induced 2'-7'- dichlorofluorescein fluorescence and protein oxidation in bovine aortic endothelial cells; ii) inhibit cytochrome C release, caspase-3 activation and DNA fragmentation; iii) inhibit H_2O_2 and lipid peroxide induced inactivation of complex I and aconitase thus preventing the production of superoxide; iv) inhibit Tranferin receptor overexpression and mitochondrial uptake of Fe thereby inhibiting apoptosis (Gow et al. 1996); and v) restore the mitochondrial membrane potential and proteasomal activity (Dhanasekaran et al. 2004). Further, the pro-oxidant effect or superoxide production by Mito-Q10 was found to be insufficient to cause any damage but led to hydrogen peroxide production and nitric oxide consumption (James et al. 2005). In spite of these results, the effect of these compounds on the reversal of damage that has already been caused by oxidative stress has not been investigated.

The antioxidant efficacy of Mito-Q10 is due to its conversion to ubiquinol by complex II of the mitochondrial respiratory chain, but its re-oxidation back to ubiquinone by complex III is ineffective. In ubiquinol form, Mito-Q10 quenches ONOO- and becomes oxidized which can be reduced by complex II to ubiquinol, making it available to quench more ONOO- (James et al. 2005).

Mito-Q10, may be effective in preventing the nitration of MnSOD, and may serve as an effective therapeutic intervention to slow the progression of AD.

Mitochondrial respiratory dysfunction and oxidative stress have been associated with many neurodegenerative diseases (Beal et al. 1995). Results obtained in this study on mitochondrial respiration using pyruvate plus malate as substrate demonstrate that in APP/PS-1 mice there is inhibition of NAD-linked state 3 respiration rate, which is mediated through complex 1 of the mitochondrial electron transport chain. RCR represents functional integrity of isolated mitochondria (Yen et al. 1999). A high value of RCR that indicates the utilization of substrates is tightly coupled to the production of ATP (Mathews et al. 1990). The "respiration injury" would predict a low coupling efficiency of the mitochondrial electron transport and an increased likelihood of electron leakage during respiration, leading to O_2-. radical formation and increased oxidative stress. Our finding is consistent with that of Kokoszka et al. (2001) who reported a decrease in state III respiratory states and the RCR of liver mitochondria from both homozygous and heterozygous knock-out mice for the gene encoding the MnSOD protein, Sod2. Cardiac mitochondria from Sod2+/- mice, which have 50% reduction in MnSOD activity, showed altered mitochondrial function as exemplified by decreased respiration by complex I and an increase in the sensitivity of the permeability transition pore induction (Van Remmen et al. 2001). Thus mitochondria from the heart (Sod2+/-) and liver (Sod-/- and Sod2+/-) show evidence of increased oxidative damage compared with mitochondria isolated from Sod2+/+ mice. Yen et al. (1999) showed that MnSOD selectively protected state 3 respiration activity through complex I substrates and prevented complex I inactivation in heart mitochondria treated with the anthracyclin antibiotic, adriamycin. These results indicate that MnSOD plays a critical role in oxidative stress responses and in maintenance of mitochondrial respiration and the lack or reduced activity of which lead to increased sensitivity of the animals to oxidative stress-induced mitochondrial damage. The decreased activity of MnSOD in APP/PS-1 mice can be implicated as a cause of decreased state 3 respiration rate seen in these mice. Our study, which shows a decline in mitochondrial respiration in aged (9 and 12 months) wild type mice, also implicates the effects of mitochondrial ROS production in the process of aging. Our findings are consistent with the studies that demonstrate a decline in respiratory function of mitochondria with age (Yen et al. 1989, Cooper et al. 1992, Wei et al. 1998) and decreased mitochondrial respiratory function in aged or

aging mice, due to deficiencies in the MnSOD (Kokoszka et al. 2001). Our results also suggest that nitrative inactivation of MnSOD may at least be in part responsible for the decline in the mitochondrial function of aging AD mice. Biochemical analyses of brain specimen from patients with AD have shown abnormalities in the components of electron transport chain, particularly in the activity of cytochrome oxidase (COX) (Maurer et al. 2000, Kish et al. 1999). Inhibition of COX could cause depressed ATP synthesis and bioenergetic impairment in AD. In addition, the decreased COX function could cause diversion of electrons from their normal pathway into reaction with molecular oxygen in the neocortex and hippocampus in AD, resulting in increased $O_2^{\cdot-}$ (Markesbery 1997). Superoxide can contribute to mitochondrial impairment by generating additional reactive species, particularly hydroxyl radical, and peroxynitrite that can inactivate mitochondrial proteins leading to further decline in mitochondrial respiration, decreased of ATP production and ultimately neuronal cell death (Eckert et al. 2003).

Although there is no consensus about the activity level of MnSOD in AD, there have been reports of reduction of SOD activity in AD frontal cortex, hippocampus and cerebellum (Richardson et al. 1993) and elevation of SOD activity in the caudate nucleus of AD (Marklund et al. 1985). But there are reports of increased nitrotyrosine immunoreactivity in neurons of AD (Good et al. 1996, Vodovotz et al. 1996). To our knowledge the identity of the nitrated proteins in the AD brain is not known. Our results showing decreased activity of MnSOD in relation to age and nitration is the first study directed to the identification of nitrated proteins in AD brain.

The mouse model used in our study has the sequence of Aβ identical to the human sequence. Further, the mutations introduced are driven by endogenous promoters of APP and PS-1 genes and expression is limited to the replacement of these two endogeneous genes and not by the expression of multiple transgenes. The amyloid pathology observed in this model is similar to that found in AD. Thus, the results obtained from this model may prove useful in unraveling the pathogenesis of AD-induced oxidative stress.

In conclusion, in this study we demonstrated an increased and accelerated deposition of Aβ in APP/PS-1 mice, increased levels of Aβ1-40/1-42, increased nitrotyrosine and subsequent inactivation of MnSOD and impaired mitochondrial respiration in APP/PS-1 mice in association with age. The increased levels of Aβ1-40/1-42, essential for aggregation and subsequent neurotoxic

properties, are observed from 6 months on. It is tempting to speculate that the increased Aβ may be the cause of alterations seen in MnSOD and the associated decrease in mitochondrial function. These changes may lead to altered function of mitochondrial permeability transition pore (Yen et al. 1989), which increases the propensity to undergo apoptosis. This is important because findings indicate that neuronal cell death associated with Aβ peptide are apoptotic in nature (Dickson et al. 2004). Thus, our studies which indicate mitochondrial dysfunction, an age-associated increase in nitration of MnSOD, and its concomitant decrease in antioxidant activity, may provide the missing link between Aβ induced oxidative stress and progression of AD.

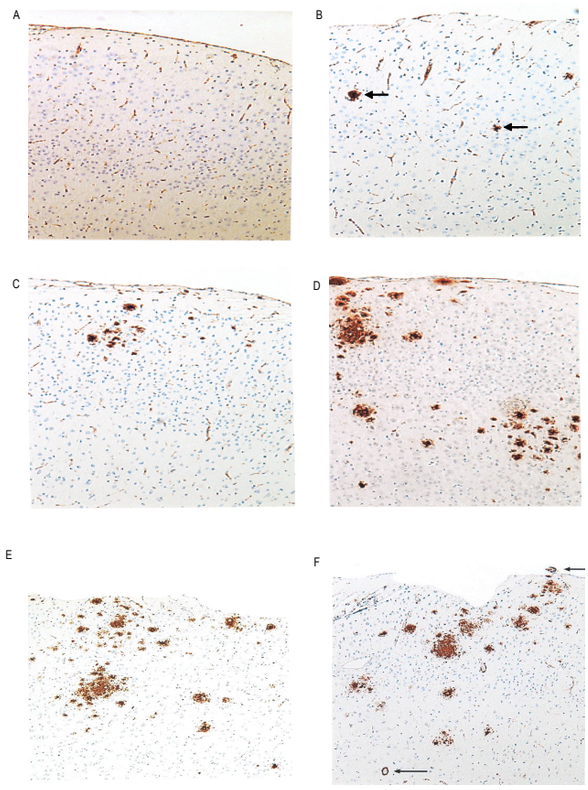

Figure 4.1: Sections of frontal cortex from APP/PS-1 mice immunostained with 10D-5 antibody for Aβ. A: 3-month old animal showing no amyloid immunostaining in cortex. B: 6-month old mouse showing rare small deposits of Aβ (arrows). C: 9-month old mouse showing increased Aβ deposits. D: 12- month old mouse demonstrating numerous variable size deposits of Aβ. E: 14-month old mouse showing numerous diffuse Aβ deposits in cortex. F: 14-month old mouse demonstrating many Aβ deposits in cortex in parenchymal and leptomeningeal vessels (arrows). Original magnifications, ×100. (From Professor William R. Merkesbery with permission)

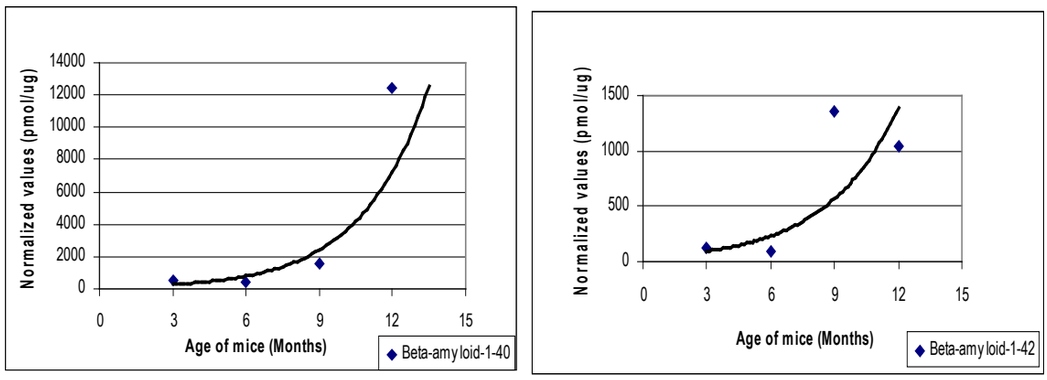

Figure 4.2: Levels of Aβ1-40 and 1-42 in APP/PS-1 mice. Aβ1-40 and Aβ1-42 levels were measured by ELISA from different groups (n = 5/group) as described in Materials and Methods section. Both species of Aβshowed an increasing trend in the levels associated with age (R2 = 0.8072 for Aβ1-40 and 0.702 for Aβ1-42). (From Michael P. Murphy, Dr. Jeffery N. Keller with permission)

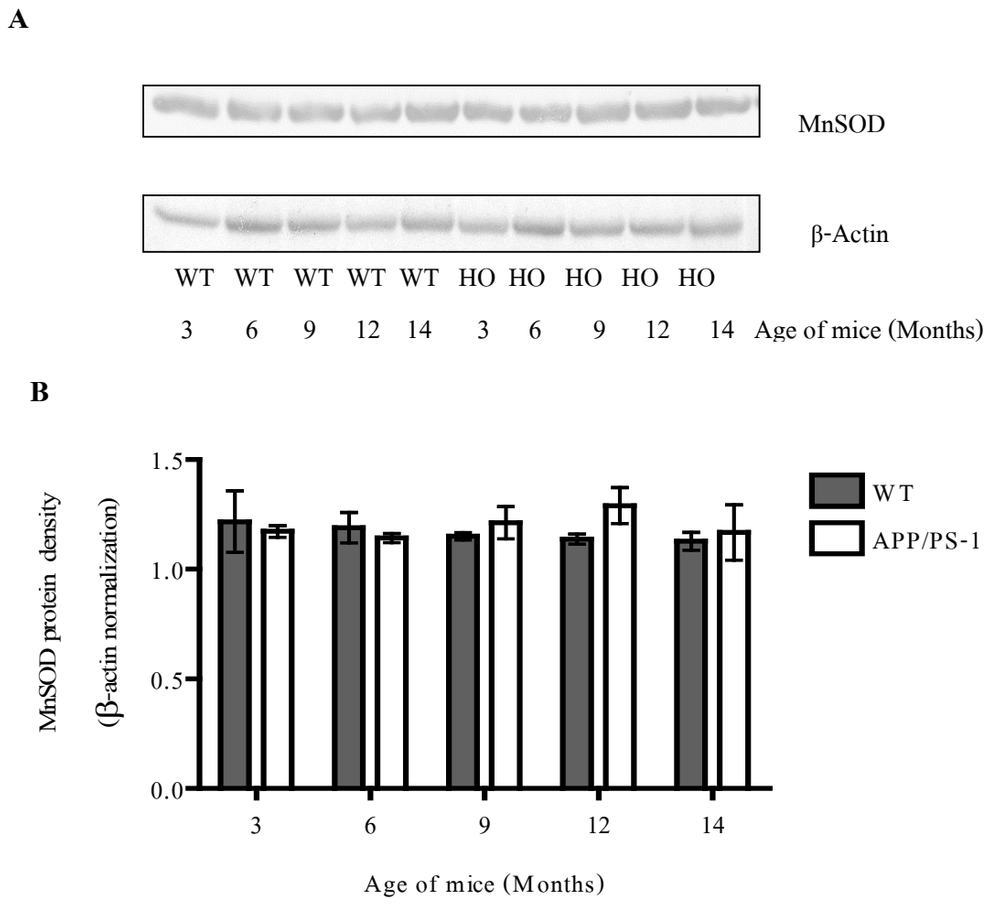

Figure 4.3: Representative (out of three) immunoblot (A) and densitometry analysis (B) showing the levels of MnSOD. Protein (30 µg) extracted from brain specimens of APP/PS-1 knock-in and wild type mice were run on a 12.5% SDS-polyacrylamide gel electrophoresis. Protein levels of MnSOD did not show significant age and genotype associated alterations. β-actin was used to normalize protein loading. WT, Wild type; HO, APP/PS-1.

A

3m 6m 9m 12m 14m 3m 6m 9m 12m 14m Positive Pellet Supernatant

WT HO control IgG

B

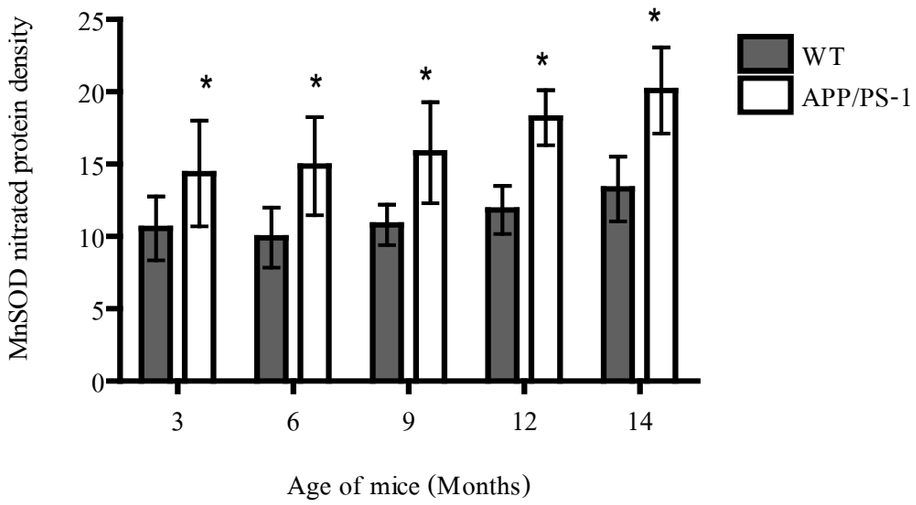

C

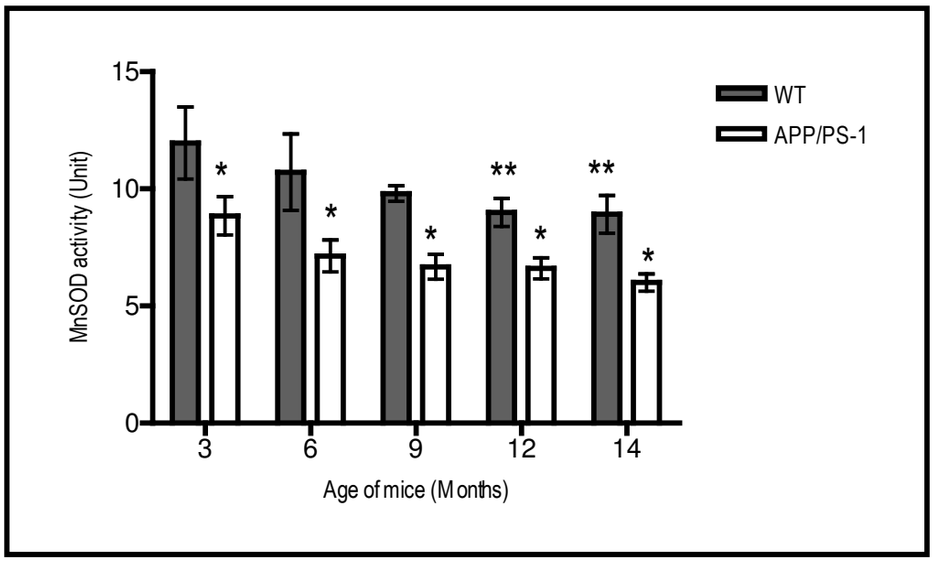

Figure 4.4: Immunoprecipitation of nitrotyrosine with MnSOD. Isolated mitochondrial protein (200 μg) was precipitated with polyclonal nitrotyrosine antibody and analyzed by Western blotting using MnSOD antibody. A, Nitrotyrosine co-immuno-precipitated with MnSOD showed that MnSOD is nitrated. WT, Wild type; HO, APP/PS-1; Positive control, Brain homogenate+ Peroxynitrite (2 μM), Pellet and Supernatant ,Pellet and Supernatant of the isolated mitochondrial protein (200 μg) precipitated with pre-immune IgG, analyzed by Western blotting using MnSOD antibody. B, Densitometric analysis and subsequent statistical analysis by 2-way ANOVA showed significant differences (*$p < 0.01$) when compared between genotypes. C, MnSOD activity in the brain specimen was measured by the nitroblue tetrazolium (NBT)-bathocuproine sulfonate (BCS) reduction inhibition method (Spitz and Oberley 1989). Statistical analysis by 2-way ANOVA showed significant age- and genotype-dependent decreases (* $p < 0.0001$) in activity of MnSOD. APP/PS-1 mice, at all ages, showed significant decreases (* $p < 0.05$) in MnSOD activity when compared with age-matched WT mice. WT mice at 12- and 14-months showed significant decrease (** $p < 0.05$) in MnSOD activity when compared with 3-month old WT mice. Immunoprecipitation and MnSOD activity was carried out in three sets of animals.

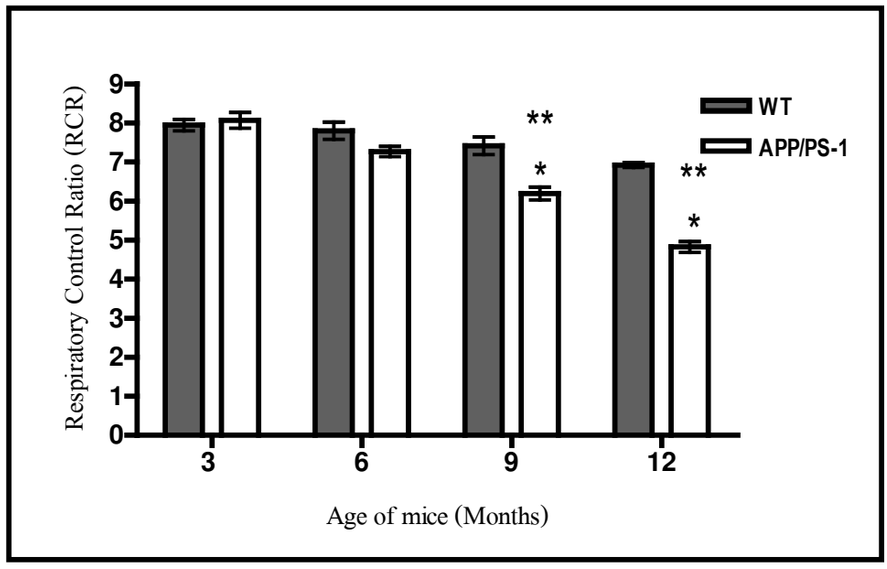

Figure 4.5: Decline in mitochondrial respiration via complex I in APP/PS-1 mice. Oxygen consumption was measured using a Clark-type electrode oxygraph. Respiratory control ratio (RCR) was calculated as the ratios between state 3 and state 2 respirations. APP/PS-1 mice at 9 and 12 months of age showed a significant decrease (* $p < 0.01$) in mitochondrial respiration when compared to its age-matched WT mice and a significant decrease (** $p < 0.001$) compared to 3-month old mice of both genotypes. Statistical analysis – two-way ANOVA followed by Newman-Keuls multiple comparisons test.